Comparative Simulation Studies of Multipacting in Higher-Order-Mode Couplers of Superconducting RF Cavities

Y.M Li,[1,2] K.X Liu,[1,*] R.L Geng[2,†]

[1]*State Key Laboratory of Nuclear Physics and Technology,*
Institute of Heavy Ion Physics, Peking University, Beijing, 100871, China.
[2]*Thomas Jefferson National Accelerator Facility, Newport News, VA 23606, U.S.A.*

Multipacting (MP) in higher-order-mode (HOM) couplers of the International Linear Collider (ILC) baseline cavity and the Continuous Electron Beam Accelerator Facility (CEBAF) 12 GeV upgrade cavity is studied by using the ACE3P suites, developed by the Advanced Computations Department at SLAC. For the ILC cavity HOM coupler, the simulation results show that resonant trajectories exist in three zones, corresponding to an accelerating gradient range of 0.6–1.6 MV/m, 21–34 MV/m, 32–35 MV/m, and > 40MV/m, respectively. For the CEBAF 12 GeV upgrade cavity HOM coupler, resonant trajectories exist in one zone, corresponding to an accelerating gradient range of 6–13 MV/m. Potential implications of these MP barriers are discussed in the context of future high energy pulsed as well as medium energy continuous wave (CW) accelerators based on superconducting radio frequency cavities. Frequency scaling of MP's predicted in HOM couplers of the ILC, CBEAF upgrade, SNS and FLASH third harmonic cavity is given and found to be in good agreement with the analytical result based on the parallel plate model.

I. INTRODUCTION

Multipacting (MP) is a phenomenon of resonant electron multiplication in which some specific inner surface areas of a radio frequency (RF) device are repeatedly bombarded by electrons which gain energy from the RF field contained in the device [1, 2]. MP was observed in superconducting radio frequency (SRF) cavities for accelerators in the 1970s and has attracted many studies since then [3, 4]. Due to the energy deposition of MP electrons at bombardment sites, the cavity wall temperature will rise. In case the SRF transition temperature is exceeded, this would lead to a thermal run away and ultimately rapid dissipation of the stored energy in the cavity. As a result, MP used to constitute a limitation to the reachable accelerating gradient in a SRF cavity. Progress has been made over the past decades in understanding and alleviating the MP problem in SRF cavities. For example, by adopting an elliptical profile in an axially symmetric cavity operated in the TM010 mode, "hard" MP's [5] in which electrons may gain energy of hundreds of eV, can be fully avoided [6, 7]. This has allowed successful applications of elliptical SRF cavities for electron acceleration (in linacs such as CEBAF, FLASH and storage rings such as TRISTAN, HERA, CESR, KEKB, and LHC etc.) as well as for proton acceleration (in linacs such as SNS).

Higher order modes (HOM) excitation in a RF cavity by charged particles has some adverse effects such as causing emittance growth of the beam under acceleration or resulting in additional heat load to the cryogenics in case of an SRF accelerator. Hence HOM damping and extraction are needed to avoid beam instability and to reduce unwanted heat load to the cryogenic system of an SRF accelerator. Various HOM dampers have been

developed and found successful applications. A commonly used HOM damper in an SRF cavity is a coaxial-type coupler, such as the one originally developed for the 1300 MHz TESLA cavity [8]. A sketch is shown in Fig.1. The TESLA-style HOM coupler has been adopted also in SRF cavities for the SNS (scaled to 805 MHz), the energy doubling of CEBAF from 6 GeV to 12 GeV (scaled to 1497 MHz), the European XFEL, and the proposed International Linear Collider (ILC).

Through systematic numerical simulation studies, the present work deals with the MP characteristics of HOM couplers of the ILC baseline cavity and the CEBAF upgrade cavity. Our studies are motivated by some recently observed experimental phenomena both at Jefferson Lab and elsewhere in TESLA-style 9-cell cavities. Those phenomena are not yet understood but suspected to be related to MP's in HOM couplers. Examples include the baking induced field emission turn-on phenomenon at a gradient of > 23 MV/m [9] and the pass-band mode excitation phenomenon with the detection of only low-energy X-rays [10]. In addition, the ILC baseline design requires an average gradient of 31.5 MV/m for cavities in operation with beam with an allowable gradient spread of ±20%. This means that an ILC cavity may need to run at a gradient of up to 38 MV/m. Due to the gradient overhead consideration, a cavity operated with beam at 38 MV/m must be tested up to 42 MV/m during its vertical qualification testing [11]. Previous simulations of MP in HOM couplers of a TESLA-type cavity were limited to a gradient of 35 MV/m [12]. Therefore the present study explores a broader gradient range of up to 47.5 MV/m. Lastly, our studies also concern MP in HOM couplers of a CEBAF upgrade cavity. Eighty of these cavities are to be ultimately installed in CEBAF to double its energy from 6 GeV to 12 GeV [13]. A detailed analysis of MP characteristics of the HOM couplers in a CEBAF upgrade cavity is still lacking. It should be noted that there are differences in the physical configurations between the HOM couplers for an ILC cavity and CEBAF upgrade cavity [14]. Therefore it is of great interest to compare the MP characteristics of the two.

II. COAXIAL-TYPE HOM COUPLER

As shown in Fig. 1, the main parts of a TESLA-style coaxial-type HOM coupler include: (1) A loop antenna for coupling the HOM power; (2) A notch filter for rejection of the power due to the accelerating mode; (3) A HOM pickup probe for extracting HOM's to an external load. The notch filter is tuned to be at resonance with the fundamental mode of the cavity so as to suppress fundamental mode coupling to the HOM pickup probe. For an ILC cavity, two HOM couplers are located with one on each side of the cavity end-group. In case of a CEBAF 12 GeV upgrade cavity, two HOM couplers are located on one side of the cavity end-group [15, 16]. The HOM couplers of SNS cavities are also based on the TESLA-type HOM coupler [17].
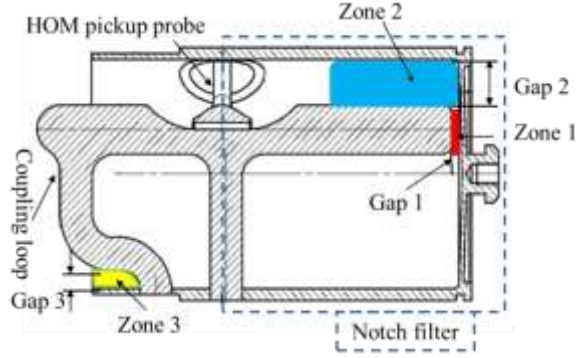
Fig. 1 TESLA-style coaxial HOM coupler. Three major parts including the coupling loop, the notch filter and the HOM pickup probe are shown. Also shown are definition of three gaps and three zones (with color) for characterization of MP.

III. SIMULATION TOOL

The electromagnetic code suites ACE3P developed at SLAC are based on high-order parallel finite element method for geometry fidelity and simulation accuracy. ACE3P includes the eigenmode solver Omega3P and the particle tracking code Track3P [18]. In our simulation studies, Omega3P was used to obtain the field distribution in the cavity and HOM couplers and Track3P was used for calculation of trajectories of MP electrons. These codes are previously used in studying MP in SRF cavities with favorable results [19, 20].

Here a brief introduction of the MP algorithm is given [21]. First, electrons are launched from specific surfaces at different RF phases. The initial velocity of the electron is perpendicular to the surface. The initial energy is fixed (typically 2 eV). The initially launched electrons follow trajectories determined by the electromagnetic fields and eventually hit the boundary of the structure. Secondary electrons are then emitted, the number of which depends on the secondary emission yield (SEY) of the boundary material and the impact energy. Tracking of electrons continues until a resonant trajectory is identified. The present study concerns predominantly the one-surface and two-surface MP. In these cases, a resonant trajectory is found when the following two criteria are met: (1) electrons return to a small area repeatedly at a nearly constant phase angle (numerically some spread in phase angle on the order of a few degrees is allowed); (2) the SEY corresponding to the impact energy is greater than unity. Typically the tracking time is long enough to ensure a pre-determined number of impacts are registered. The kinetic energy of electrons upon each impact is also registered for each involved surface. For resonant electrons hitting the same surface, their impact energy is average and plotted against the acceleration gradient. In our simulation, the niobium SEY curve is shown in Fig. 2 [22]. The SEY includes the contribution from true secondary electrons as well as reflected electrons and re-diffused electrons. The effect of SEY enhancement due to glance incidence is presently not considered in the code. A very useful concept of enhanced counter function (ECF) is used for analyzing the MP data. The ECF is a measure of total number of electrons after several RF periods.
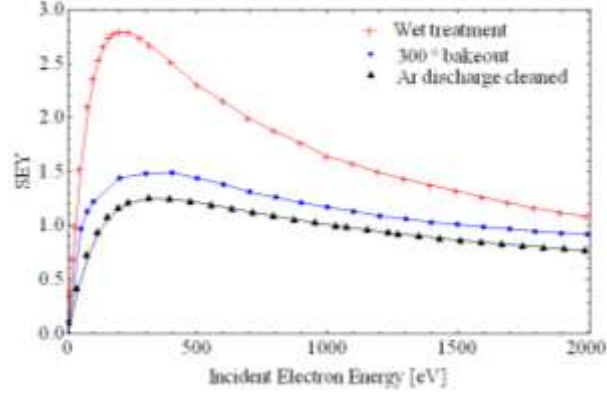
Fig. 2 Secondary emission yield curves for niobium surfaces of various treatments.

IV. SIMULATION RESULTS

A. ILC cavity HOM couplers

For the purpose of MP simulations in HOM couplers, we adopt a simplified model as shown in Fig. 3. It consists of a one-cell TESLA cavity (end half-cell shape) and a HOM coupler. The validity of this model is justified in viewing that the electromagnetic field configuration in the HOM coupler region is uniquely proportional to the field in the end cell of a 9-cell cavity. The subtle difference between the center half-cell and the end half-cells is expected to introduce negligible effect for the MP characteristics in HOM couplers.
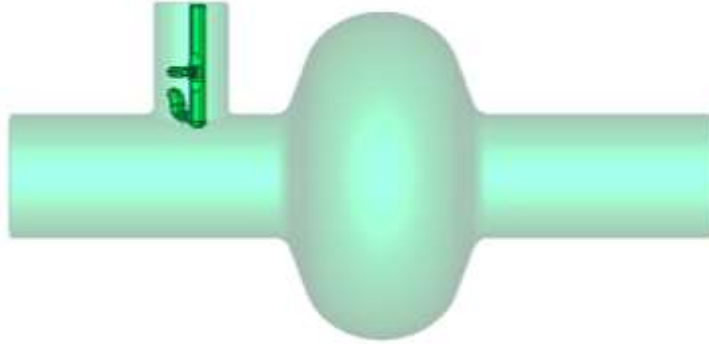

Fig. 3 One-cell cavity model for MP simulations in an ILC cavity.

The notch filter RF behavior is very sensitive to the notch gap. Before the MP simulation, the notch frequency has to be tuned to the cavity resonance frequency. Details about tuning the notch gap can be found in Ref. [23]. The notch filter gap in our model is tuned to 1.41 mm.

The RF electric field distribution of the fundamental mode in the HOM can is shown in Fig. 4. The ratio of the local peak electric field E_{pt} at the tip of the HOM antenna to the accelerating gradient E_{pt}/E_{acc} is ∼ 27%. At an accelerating gradient of 42 MV/m, the peak electric field in the HOM coupler region amounts to > 11 MV/m, which is clearly not a trivial field in terms of MP or even field emission consideration.
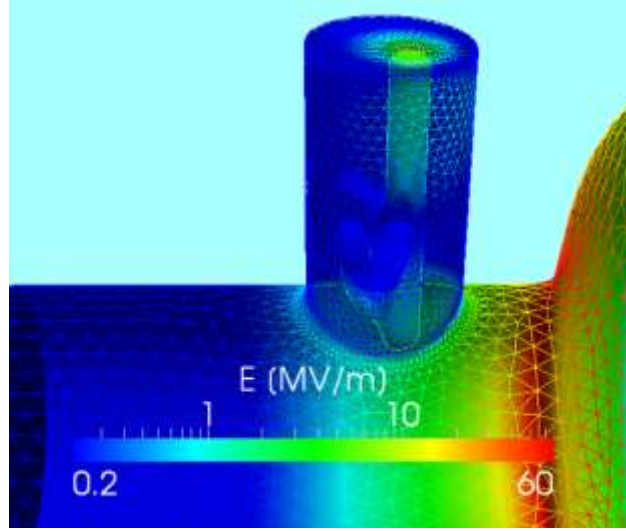
Fig.4 Contour of the electric field in a TESLA-style HOM coupler ($E_{acc} = 31.5 \, \text{MV/m}$). Rapid decay of the electric field of the fundamental mode from the end-cell (at right) into the beam tube (at left) is evident. The peak local electric field at the tip of the coupling loop is 27% of the accelerating gradient. The peak electric field across the gap (Gap 1 in Fig. 1) between the antenna and the bottom of the HOM can is 19% of the accelerating gradient.

The initial electrons are launch from the whole inner surface of the HOM coupler. After comprehensive survey, we found MP's in three zones as indicated in Fig. 1. Detailed information is given in the following paragraphs.

The ratio of the peak electric field E_{pg} across the gap in Zone 1 (between the HOM antenna and the HOM can, see Fig. 1) to the accelerating gradient E_{pg}/E_{acc} is ~ 19%. The RF magnetic field vanishes in Zone 1. As a result, the MP in Zone 1 can be treated as the well-known configuration of a pair of parallel plates, with an average gap of 1.41 mm and slope angle of 2°. Our numerical simulation results show that the 1st-order MP takes place at an accelerating gradient in the range of 0.6–1.6 MV/m. The impact energy of the MP electrons is in the range of 50–325 eV as shown in Fig. 5(a). The ECF (for sustained impacting of 20 RF periods) for different SEY's are given in Fig. 5(b). Clearly, even for the case of "clean" niobium surface, there is a good chance of MP in Zone 1.

Typical electron trajectories of MP electrons are given in Fig. 5(c). It can be seen that the MP in Zone 1 is not a fixed two-point MP between two parallel-plates. Due to the fringe field effect resulted from the asymmetric structure of the HOM coupler, MP electrons drift away from the gap space and ultimately fall off the square area of the inner conductor.
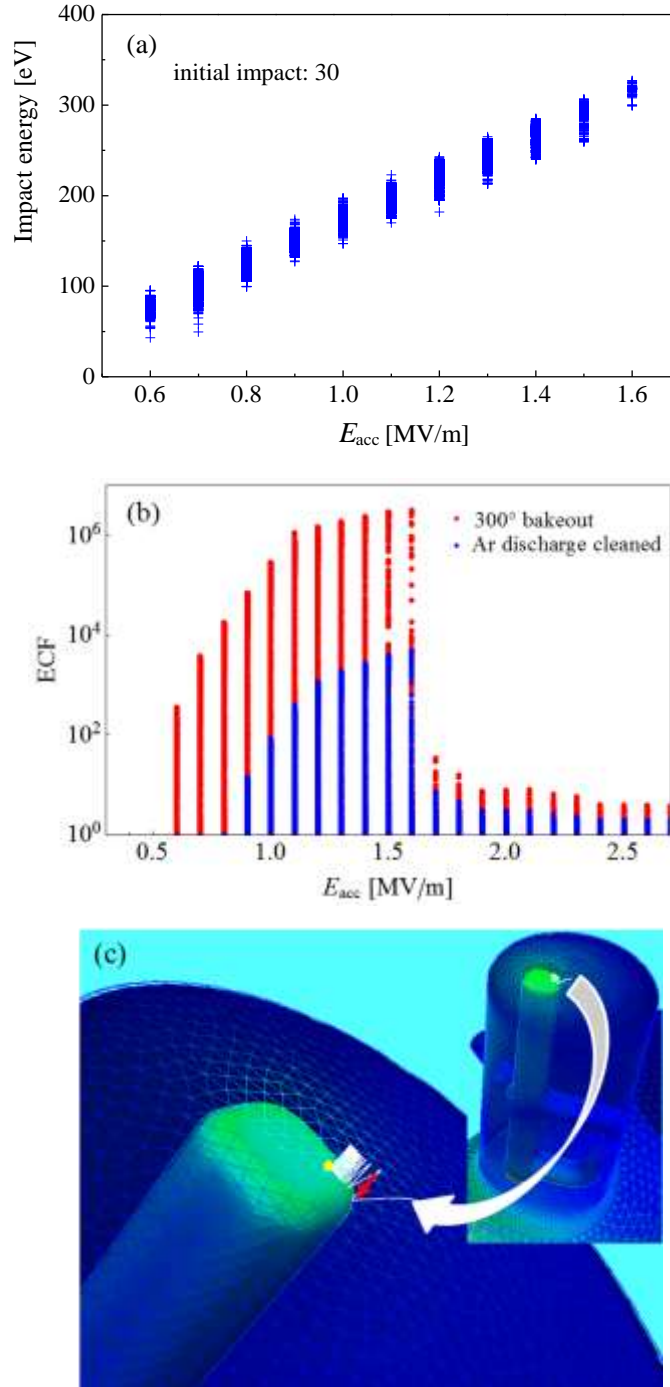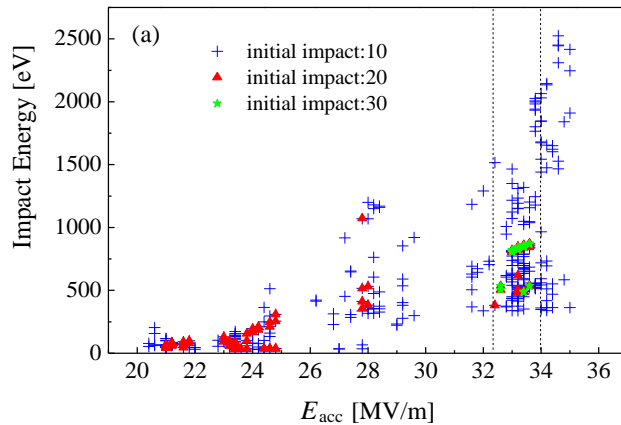
Fig. 5 Characteristics of Zone 1 MP: (a) Electron impact energy. (b) Enhancement counter function after impacting for 20 RF periods. (c) Typical electron trajectory. The emission site is indicated by the yellow dot. The movement direction of the MP electron is indicated by red arrows. Finally, the emission electron slips out the square area of the inner conductor.

In Zone 2, the gap between the inner conductor and the HOM can is 8.2 mm (Gap2 in Fig.1) by design. Resonant trajectories exist in Zone 2 for an accelerating gradient range of 21−35 MV/m. The electron impact energy for the sustained impacting of 10, 20, and 30 times is given in Fig. 6(a). As can be seen, sustained

impacting for 10 times is possible over a broad gradient range of 21–35 MV/m with an impacting energy in the range of 40–2500 eV. However, sustained impacting for 20 times is only possible for a reduced gradient range of 21–25 MV/m, around 28 MV/m and 32–34 MV/m with an impacting energy in the range of 40–1100 eV. The gradient range for which sustained impacting for 30 times is further narrowed to 32–34 MV/m with an impacting energy in the range of 400–800 eV. The enhanced counter function (for 20 RF periods) for different SEY's is given in Fig. 6(b). Detailed analysis of simulation results shows that Zone 2 MP can be divided into two groups. The first MP is from 21–30 MV/m with typical electron trajectories as shown in Fig. 6(c). Due to its complex nature of the trajectories, we term this type of MP as "corner MP", in which more than two points are involved and perhaps involves some level of hybrid between a one-point MP and a two-point MP. As a result, the MP electron will ultimately slip out of the resonant phase after some number of impacts and ultimately get lost. This kind of "quasi resonant" barrier typically is not expected to be observable for a clean surface with a low SEY because the growth in electron density is limited by multiplication time. Even if the surface cleanliness is less ideal, such a barrier is expected to be only observable at the initial power rise during RF testing. The second MP is from 32–34 MV/m and the typical electron trajectories are shown in Fig. 6(d). This is a 1st-order one-point MP with resonant trajectories that sustain even after 30 impacts. In addition, as shown in Fig. 6(a), the impact energy for this MP is in the range of 400–800eV. As a result, this kind of "hard" barrier can persist even after extended "conditioning" by deliberately parking the RF field at the barrier gradients.
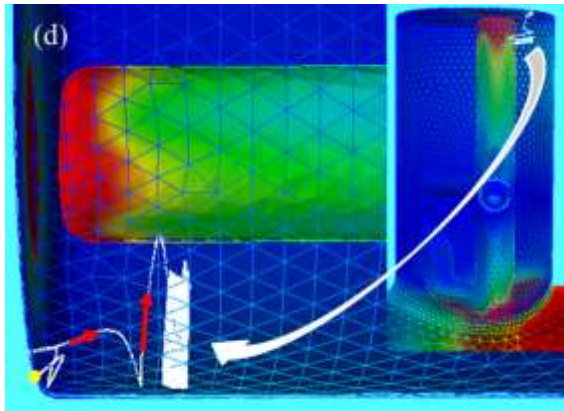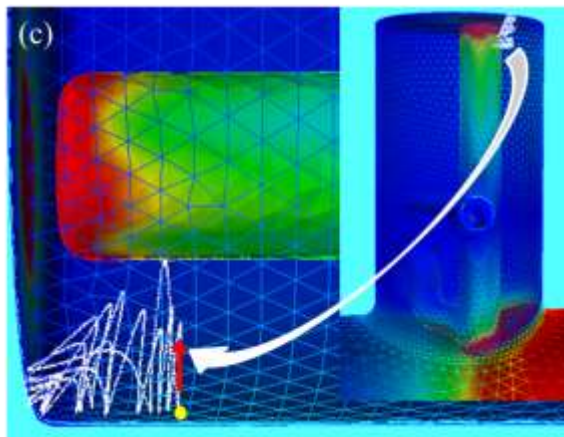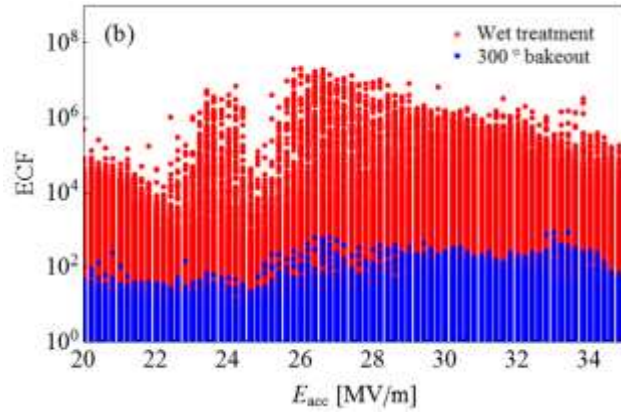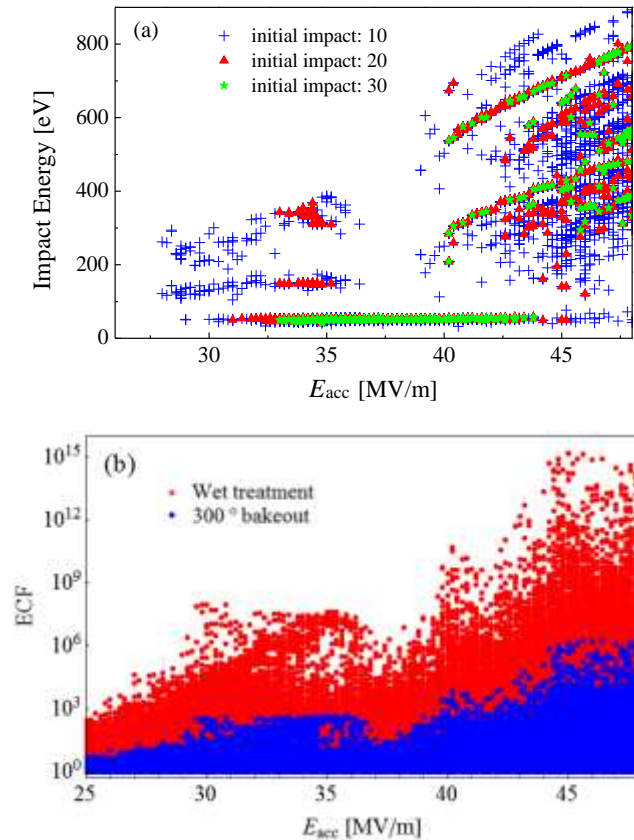
Fig. 6 Characteristics of Zone 2 MP: (a) Electron impact energy. (b) ECF after impacting for 20 RF periods. (c) Typical electron trajectories of "quasi resonant" MP for gradients in the range of 21−30 MV/m. The initial emission electron is from the yellow dot position moving forward with the red arrow direction. The emission electrons will ultimately slip out of the resonant phase after some number of impacts and ultimately get lost. (d) Typical electron trajectories of "hard" MP for

gradients in the range of 32–35 MV/m. The initial emission electron is from the yellow dot position moving forward with the direction shown in the figure. Finally, the emission electrons form a stale trajectory.

In Zone 3, resonant trajectories exist for an accelerating gradient in the range of 32–35 MV/m and >40 MV/m. The electron impact energy for sustained impacting of 10, 20, and 30 times is given in Fig. 7 (a). The gradient range for sustained MP becomes narrowed as the impact number increases. The ECF after 20 RF periods are shown in Fig. 7(b). Through detailed analysis, the resonant electrons are found to impact surfaces in two regions shown in Fig. 7 (c). The electron impact energy in the upper region tends to be less than 100 eV. This barrier is a two-surface 3rd -order MP which involves the inner surface of the HOM can and the outer surface of the HOM loop antenna. Typical upper region electron (around 50eV) trajectories (which can persist even after 30 RF cycles) are shown in Fig. 7(d). The electron impact energy in the lower region falls in the range of 250–800 eV. This barrier is two-surface 3rd -order MP for gradients below 40 MV/m and two-surface 1st -order MP with gradient above 40 MV/m. Typical high energy MP electron trajectories (in the lower region) are shown in Fig. 7 (e), showing electrons drafting out of resonant phase eventually after some number of impacts. Due to the high impacting energy, the hard MP barrier at > 40 MV/m is likely to persist even after sustained RF conditioning because of a high SEY (see Fig. 2).
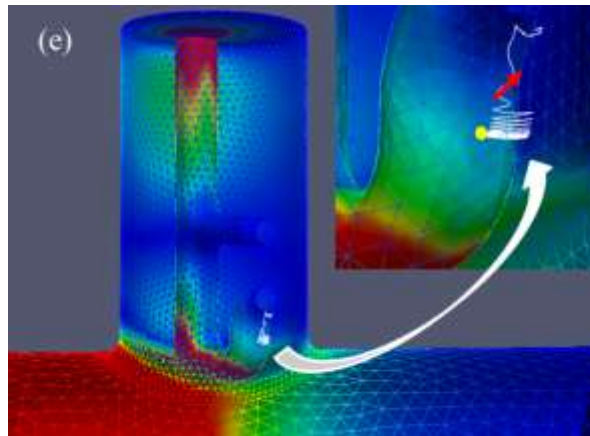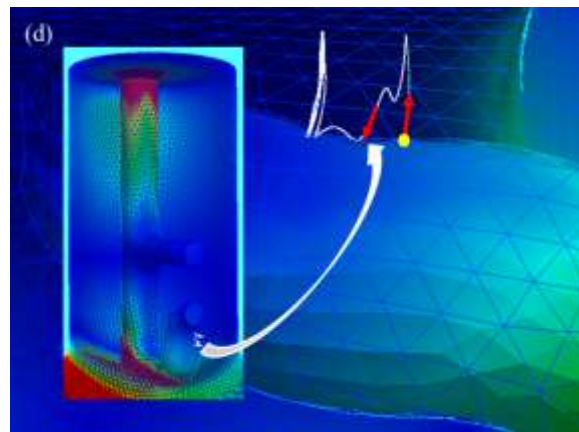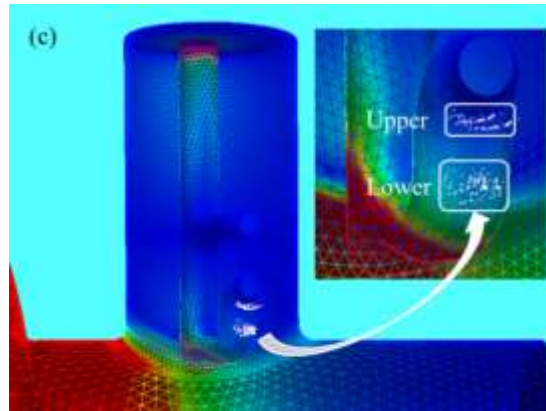
Fig. 7 Characteristics of Zone 3 MP: (a) Electron impact energy. (b) Enhancement counter function after 20 RF periods. (c) Two MP regions. (d) Typical low impact energy resonant electron (upper region) trajectories. The emission site is indicated by the yellow dot. The initial movement direction of the MP electron is indicated by red arrows. The ultimate resonant trajectory between the two surfaces with impact energy of ~50eV is also shown. (e) Typical high impact energy resonant electron (lower region) trajectories. The MP electron ultimately slips out of resonance.

B. CEBAF 12 GeV Upgrade Cavity HOM Coupler

The HOM couplers in a CEBAF 12 GeV upgrade cavity, as shown in Fig. 8, are based on the TESLA-type HOM coupler design. In comparison to the ILC cavity, the arrangement of the HOM couplers is different: (1) Two HOM couplers are placed on one side of the cavity; (2) The HOM antenna tip is farther away from the end-cell cavity. As a result, the coupling of fundamental mode between the HOM couplers and the end cell is reduced. This reduces the HOM heating and is understood to be an important change for the CW operation of these cavities [14]. The ratio of the local peak electric field at the tip of the HOM antenna to the accelerating gradient E_{pt}/E_{acc} is ~ 8% (27% for the ILC cavity). The ratio of the peak electric field across the gap in Zone 1 to the accelerating gradient E_{pg}/E_{acc} is ~ 4.1% (19% for the ILC cavity).
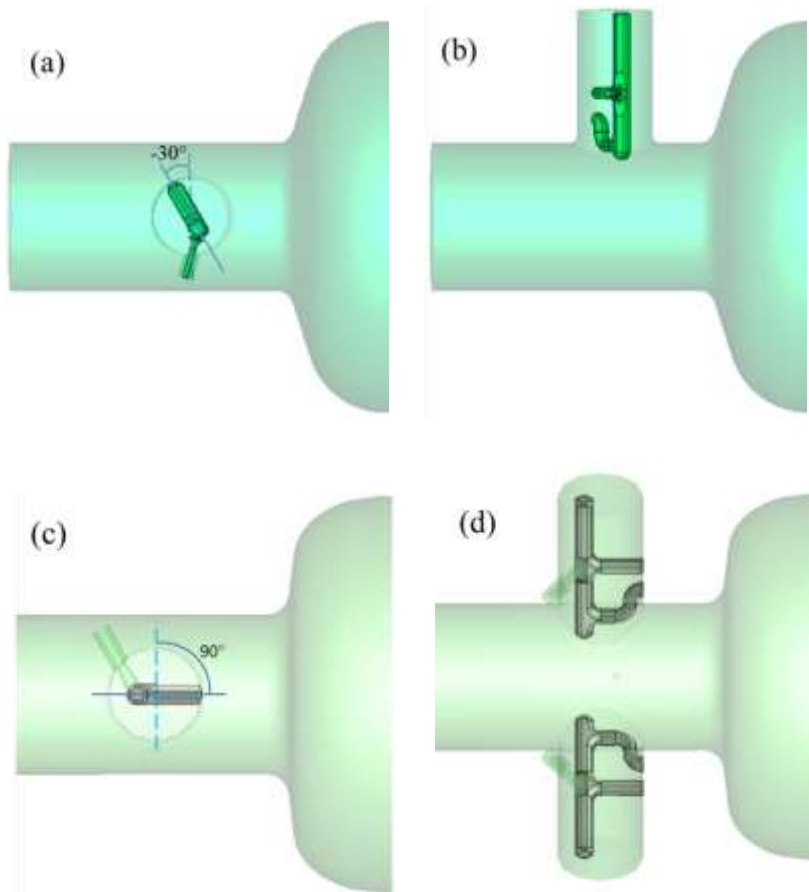

Fig. 8 Comparison of HOM couplers in ILC cavity (a) & (b) and in CEBAF 12Gev upgrade cavity (c) & (d). The angle between HOM coupler plane and the plane vertical to the cavity axis is -30° in ILC cavity and 90° in CEBAF cavity. The ILC cavity has two HOM couplers, one each at two end-groups with an angular displacement of 115° with respect to each other

when viewed along the cavity axis direction. The CEBAF upgrade cavity has two HOM couplers, both at the same end-group with an angular displacement of 115° when viewed along the cavity axis direction.

Simulation results show that resonant trajectories exist in Zone 1 for an accelerating gradient in the range of 6–13 MV/m. In this region, the gap between the HOM antenna and HOM can is tuned to 1.79 mm. The electron impact energy is shown in Fig.9. This simulation result agrees well with the analytical prediction for a two-surface MP across a pair of parallel plates [24]. This MP barrier corresponds to the one for the gradient range of 0.6–1.6 MV/m in an ILC cavity.

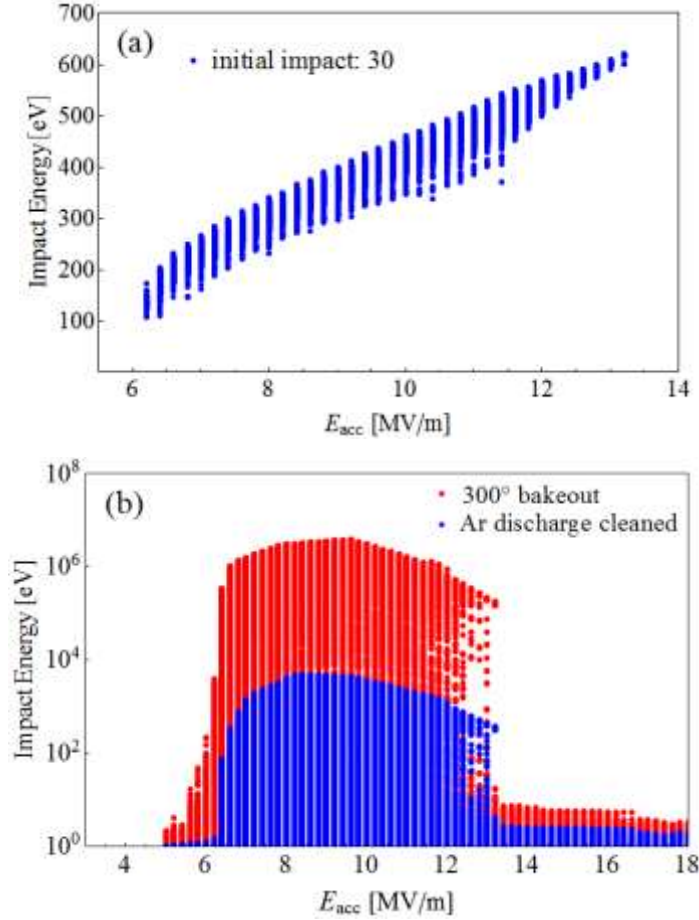Fig. 9 Characteristics of Zone 1 MP in the HOM coupler of a CEBAF upgrade cavity: (a) Electron impact energy, (b) ECF after 20 RF periods.

No MP is identified in Zone 2 or Zone 3 up to a gradient of 30 MV/m studied in this work (the operating gradient for CEBAF upgrade cavities is 19.2 MV/m).

V. DISCUSSIONS

A. Overview and comparison of MP in HOM coupler of ILC and CEBAF upgrade cavity

The MP characteristics of the TESLA cavity HOM couplers were numerically studied previously by Gonin et al [12]. Those work predicted two barriers, one at E_{acc} 1.1–1.7 MV/m in Zone 1 and the other at E_{acc} ~ 33.8 MV/m in Zone 2. These results were compared with the available experimental data. It was stated that a good agreement was observed between the simulation results and the experimental data. More recently, new evidence about Zone 1 MP was revealed by Kostin et al during the XFEL prototype module tests. Their experimental result demonstrated the existence of a MP barrier at E_{acc} 1.1 MV/m. Numerical simulation studies were also carried out, predicting a MP barrier in Zone 1 at a gradient in the range of 1.5–1.8 MV/m [25].

A summary of those prior results and our new simulation results is given in Fig.10. In addition, the analytical result base on the parallel-plate model is also shown. From Ref [24], the two-surface 1st-order MP occurs in the gradient range between the lower bound E_{min},

$$E_{min} = \frac{m\omega^2 d}{\sqrt{4+\pi^2}e} ,$$

and the upper bound E_{max},

$$E_{max} = \frac{m\omega^2 d}{2e} ,$$

where e is the electron charge and m the electron mass, d is the gap between surfaces.

It should be mentioned that there is a slight difference in the Zone 1 gap length as used by different workers. In our model, the nominal notch filter gap 1.73 mm is tuned to 1.41 mm for reasons given in Sec. IV A. No tuning attempt was reported in Ref.[12, 25] where the nominal gap length 1.73 mm was used instead. This results in a higher E_{acc} (more than ~ 50%) for the same Zone 1 MP barrier by Gonin and Kostin as compared to the present work.
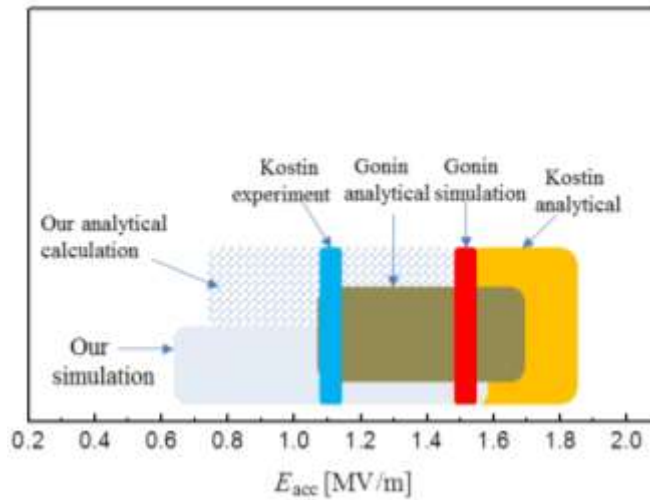
Fig.10 Summary of Zone 1 MP in the TESLA-style cavity HOM coupler. The Kostin experiment data did not give the MP field range in Ref [25]. So we use a narrow bar to represent the data point. The gradient width of Goin simulation result was also not reported. A narrow bar was used to represent the data point

Besides the Zone 1 MP at E_{acc} 0.6–1.6 MV/m, our simulations also predicted MP's over a broad gradient range from 21 to more than 45 MV/m in Zone 2 and Zone 3 in ILC cavities. It must be mentioned that most of the predicted MP's in Zone 2 and Zone 3 are "quasi resonant" barriers, namely the resonant impact is able to last for only certain periods of time. Practically, these barriers are not expected to be observable unless the effective SEY of the surface is very high. Nevertheless, even a fleeting MP could cause a burst of gas desorption from the surface in the HOM coupler. In turn, re-condensation of gases on the high electric field region near iris could trigger field emission. This might be one explanation to the experimentally observed phenomenon of baking induced field emission turn-on at a gradient of > 23 MV/m in electropolished ILC cavities [9]. Further studies of baking effect on the SEY of electropolished niobium surfaces are needed to confirm this scenario.

More importantly, our simulations predict two "hard" MP barriers, one in Zone 2 at a gradient in the range of 32–34 MV/m and the other in Zone 3 at >40 MV/m. Previously, Gonin et al predicted a MP barrier at E_{acc} ~ 33.8 MV/m in Zone 2, which is in agreement with our prediction at 32-34 MV/m. We predict *a new barrier* at > 40 MV/m. Reports on experimental observation of these predicted MP's are still scarce, suggesting these narrow barriers may be sensitive to the detailed dimension of the actual cavity and the HOM coupler. Nevertheless, as the ILC baseline design average gradient is 31.5 MV/m, which is rather close to the predicted Zone 2 MP, further experimental studies of this MP barrier are needed due to its significance to the beam operation of ILC cavities. For ILC 1 TeV upgrade, higher gradients are needed. This pushes the cavity toward the 50 MV/m regime. Our work suggests that MP in the HOM couplers is a potential limit to the achievable gradient in a full-scale TESLA-style cavity. Practically, some full-scale 9-cell cavities have reached a gradient of > 40 MV/m. The record gradient is 45 MV/m [26]. It is therefore possible to experimentally study the predicted MP barrier in Zone 3 of the HOM coupler in a TESLA-style cavity.

Our simulation also predicts a MP barrier in the gradient range of 6–13 MV/m in Zone 1 of a CEBAF upgrade cavity. Till now, all eighty cavities for CEBAF 12 GeV upgrade have completed vertical testing and no hard barrier was observed during cryogenic vertical tests. However, some high radiation starting at a gradient as low as 10 MV/m was observed in some cavities during horizontal tests in cryomodules. Further investigation with regard to the possible role of the Zone 1 MP in these cavity behaviors would be interesting.

B. MP in HOM coupler of cavities at other frequencies

MP in HOM couplers of cavities at other frequencies has been previously observed and studied. In this paper, further simulation studies of two examples have been carried out. This includes the SNS high-beta cavity and the

original FLASH third harmonic cavity. A frequency scaling attempt is herein made to analyze the MP behaviors in HOM couplers of cavities at a variety of frequencies.

During the commissioning and operation of the SNS superconducting linac, the high-beta 805 MHz cavities exhibited MP from 9.5 to 18.6 MV/m and abnormal signals originated from the HOM coupler were observed. Simulations done by Gonin and coworker using ANALYST showed MP from 10 to 26 MV/m in Zone 3 [12]. Our simulation results predict two barriers in Zone 3 at gradient 11-19 MV/m (3rd-order MP) and 25-35MV/m (1st-order MP), respectively. There is a reasonably good agreement between the first barrier we predict and previous experiment and simulation results. The second barrier we predict is above the experimentally achieved gradient, preventing direct comparison.

MP barriers in Zone 1 and Zone 3 were observed also in HOM couplers of the original 3.9 GHz 9-cell cavity. During the high power test of the #2 cavity, thermal breakdown was observed in the HOM coupler with the first barrier occurring at about 1–2 MV/m and the second wider and stronger barrier from 12 to 19 MV/m [27]. Simulation result indicated that the barrier at 1–2 MV/m is MP in zone 1 and the barrier at 12–19 MV/m is MP in zone 3. Simulations done by Gonin and coworker predicted a MP barrier at 0.7 MV/m in Zone 1 and another barrier at 11–18 MV/m in Zone 3. Our simulation results predict two barriers, one at 0.6 MV/m in Zone 1 and in the other at 10-30 MV/m in Zone 3, respectively. There is a good agreement between MP barriers we predict and previous experiment and simulation results. The highest barrier we predict is above the experimentally achieved gradient. It should be mentioned that the original HOM coupler in the third harmonic cavity was ultimately redesigned and MP was successfully avoided [27].

C. Zone 1 MP frequency scaling

The electric field dominates in Zone 1 of the ILC cavity. As can be seen in the fllowing, the two-surface MP model is suitable for analyzing Zone 1 over a broad frequency range. To study the frequency scaling, a series of cavities were scaled from a 1.3GHz TESLA-type one-cell cavity. The notch filter is confirmed to work still for the scaled cavities. The frequency scaling of the Zone 1 MP f is shown in Fig.11. The frequency scaling of the MP barrier are characterized by the range of $E_p/\omega^2 d$, where E_p is the local peak electric field, ω the angular RF frequency, and d the gap dimension across the two local areas bombarded by MP electrons. As indicated earlier in Section V.A, MP in Zone 1 can be analytically treated as two-surface MP based on the parallel-plate model, $\frac{m\omega^2 d}{\sqrt{4+\pi^2 e}} < E_p < \frac{m\omega^2 d}{2e}$. The lower and upper bound of the analytical prediction are shown as dashed lines in Fig. 11. It can be seen that the simulation results agreed fairly very well with the analytical result over a broad frequency range. A summary of the Zone 1 MP parameters of the scaled ILC cavities including the local electric field and the local gap separation is given in table 1.
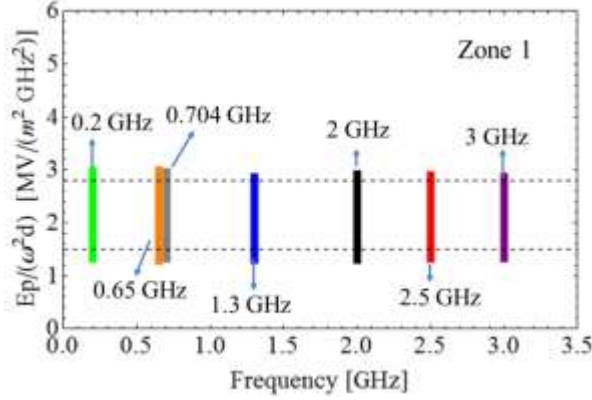
Fig.11 Frequency scaling of Zone 1 MP in HOM couplers of scaled TESLA-type cavities. The dashed lines are the lower and upper bound from the analytical prediction based on the parallel-plate model.

Table 1. The local peak electric field E_p and local gap d of Zone 1 MP in scaled TESLA-type cavities. E_{acc} is the corresponding acceleration gradient

Freq [GHz]	E_{acc} [MV/m]	Ep [MV/m]	d [mm]
0.2	0.1-0.24	0.019-0.043	9.165
0.65	0.3-0.7	0.06-0.14	2.82
0.704	0.32-0.72	0.067-0.15	2.604
1.3	0.6-1.6	0.15-0.33	1.41
2	1.0-2.2	0.19-0.42	0.917
2.5	1.2-2.8	0.24-0.53	0.733
3	1.4-3.2	0.29-0.62	0.611

Our new simulations of MP in real cavities confirm the existence of MP in Zone 1 of the HOM coupler in the original 3.9 GHz cavity. For the SNS high-beta 805 MHz cavity, no Zone 1 MP is predicted because of the low impact energy in the range of 5–40 eV. Altogether, Zone 1 MP for real cavities including the 1.3 GHz ILC cavity, 1.5 GHz CEBAF upgrade cavity, and 3.9 GHz cavity is summarized in Fig. 12. Also shown in Fig. 12 is the frequency scaling of the MP barrier as characterized by the range of $E_p/\omega^2 d$. Again, the simulation results are found to agree fairly very well with the analytical result over a broad frequency range. The Zone 1 MP parameters of the ILC, CEBAF, 3.9 GHz cavities are given in table 2.
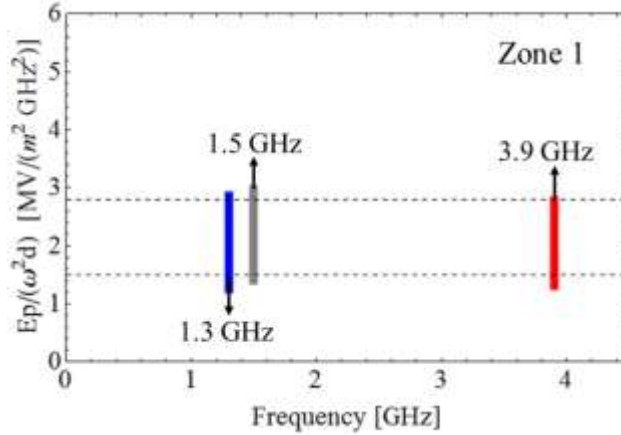
Fig.12 Frequency scaling of Zone 1 MP in HOM couplers of real cavities including the 1.3 GHz ILC cavity, 1.5 GHz CEBAF upgrade cavity, and original 3.9 GHz third harmonic cavity. The dashed lines are the lower and upper bound from the analytical prediction based on the parallel-plate model.

Table.2 The Zone 1 MP parameters of the ILC, CEBAF, 3.9GHz cavities

Freq [GHz]	E_{acc} [MV/m]	Ep [MV/m]	d [mm]
1.3	0.6-1.6	0.15-0.33	1.41
1.5	6-13	0.228-0.472	1.79
3.9	0.55-0.65	0.472-1	0.6

D. Zone 3 MP frequency scaling

Unlike Zone 1, where a gap is formed by two flat surfaces, Zone 3 is defined by more complicated surfaces. For the ILC, CEBAF upgrade and SNS HOM coupler, the cross section of the HOM loop antenna has a race-track shape. For the original 3.9 GHz HOM coupler, the cross section has a circular shape (see Fig. 13). The inner surface of the HOM can and the outer surface of the HOM loop antenna forms a two-surface region where MP is possible. From simulations, it is understood that the space occupied by resonant trajectories depends on the gradient. MP starts from region A at the MP onset gradient and moves toward region B with an increasing gradient (Fig.14).
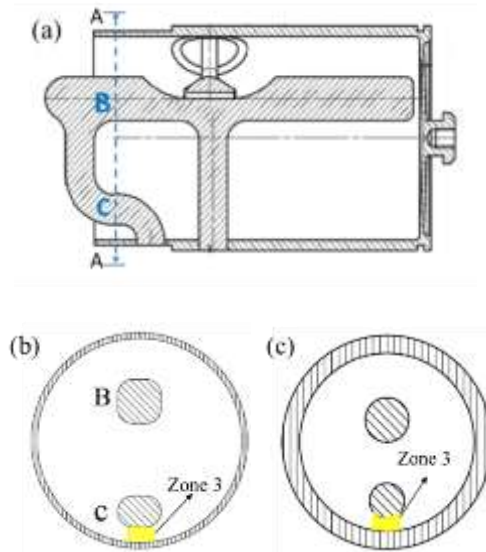
Fig. 13 (a) TESLA-style coaxial HOM coupler with sectioning line AA. (b) Cross section of ILC HOM coupler showing race-track shaped HOM loop antenna. (c) Cross section of the 3.9 GHz original HOM coupler showing circular shaped HOM loop antenna.
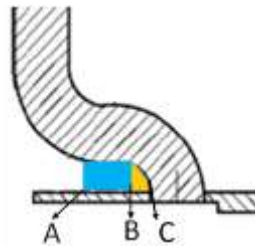

Fig.14 Space occupied by two-surface MP in Zone 3. MP starts from region A at the onset gradient and moves toward region B with an increasing gradient in ILC, CEBAF and SNS cavity. For 3.9 GHz original HOM coupler, the MP starts from A and moves toward C.

The frequency scaling of the Zone 3 MP for scaled TESLA-shape cavities is shown in Fig.15. Table 3 gives parameters of Zone 3 1st-order MP for the scaled TESLA-shape cavities. It should be noted that the scaled cavities are only for the purpose of analyzing the frequency scaling of Zone 3 MP. HOM damping is not considered. It should be also noted that the broad gradient range covered by our simulation concerns only the MP dynamics for the completeness of the understanding. In reality, there are physical limits (such as the critical RF field of the superconductor) prohibiting a cavity from reaching a field beyond a threshold. From Fig.15, we can see that the simulation results agreed fairly well with the two-surface MP analytical result over a broad frequency range.
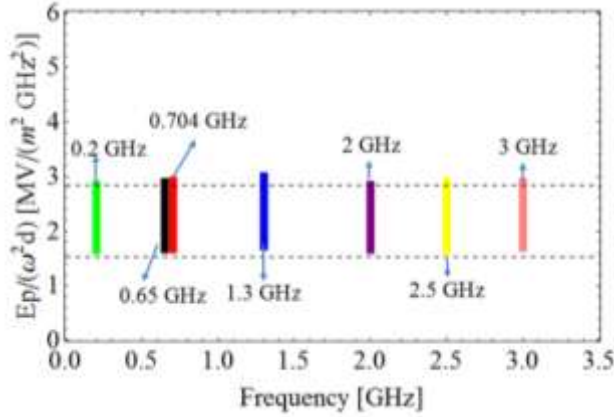
Fig.15 Frequency scaling of Zone 3 MP for scaled TESLA-type cavities.

Table 3. The local peak electric field E_p and local gap d of Zone 3 MP
in scaled TESLA-type cavities. E_{acc} is the corresponding acceleration
gradient

Freq [GHz]	Eacc [MV/m]	Ep [MV/m]	d [mm]
0.2	7–22	0.051–0.088	19.5
0.65	23–70	0.167–0.29	6
0.704	26–75	0.181–0.317	5.54
1.3	40–140	0.345–0.602	3
2	70–218	0.511–0.877	1.95
2.5	84–300	0.639–1.12	1.56
3	105–340	0.785–1.34	1.3

Next we will show that the frequency scaling of Zone 3 MP can be extended to other existing real cavities including SNS cavity (805 MHz), CEBAF upgrade cavity (1.497 GHz) and 3.9 GHz cavity. The results are shown in Fig.16. It should be noted that, for the purpose of frequency scaling, the simulation of Zone 3 MP for the CEBAF upgrade cavity is extended well beyond the practical gradient range. The normalized local electric field $E_p/(\omega^2 d)$ ranges from 1.5 to 3.1 $MV/(m^2 GHz^2)$. It should be pointed out that the lower region (above 100 eV impact energy, see Fig.7 (a) & (c)) MP is only possible in the space between line A and B (Fig. 13) where the gap separation is fixed in case of ILC, CEBAF upgrade and SNS cavities; whereas in case of the 3.9 GHz cavity, the MP develops not only in the above region but also in regions beyond line B where the gap separation varies as the gradient is further raised. A summary of the Zone 3 MP parameters including the local electric field and the local gap separation is given in table 4.
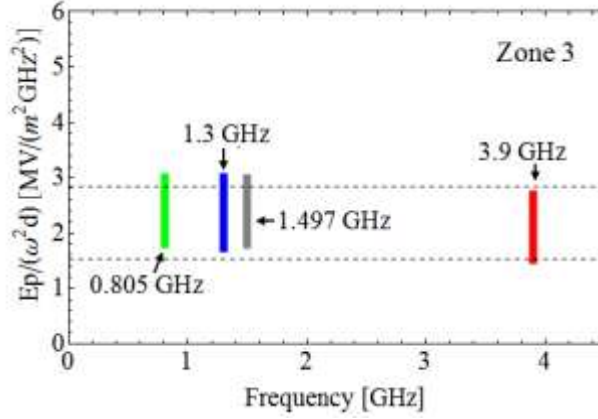
Fig.16 Frequency scaling of Zone 3 MP in HOM couplers of real cavities. The dashed lines are the lower and upper bound for analytical prediction for two-plane 1st-order MP based on the parallel-plate model.

Table 4. Summary of the local peak electric field E_p and local gap d of Zone 3 MP in HOM couplers of different real cavities. E_{acc} is the corresponding acceleration gradient.

	E_{acc} [MV/m]	E_P [MV/m]	d [mm]
ILC	40–140	0.34–0.602	3
SNS high-beta	25–35	0.27–0.44	5.83
3.9 GHz	10–30	2.3–0.43	1.4–0.48
CEBAF-Upgrade	43–113	0.47–0.79	3.13

From simulation result, "corner MP" is found in Zone 2 from 133 MV/m to 155 MV/m (for theoretical MP study) in CEBAF upgrade cavity. No MP is found in Zone 2 for 3.9GHz cavity. For ILC cavity, the MP is "corner MP" or one point MP. No scaling law is found for MP in Zone 2.

E. Discussion of MP modeling

The initial energy of the emitted electrons can be varied changed (the default value is 2 eV). In our simulations, 3rd-order MP is found in Zone 3 in the ILC cavity, CEBAF upgrade cavity and SNS cavity with impact energy of around 50 eV. The impact energy increases to 80 eV when the initial energy is set to 5 eV.

Due to the fact that the initial energy of MP electrons is not very high, the magnetic force is much less compared to the electric force ($\left| q\vec{v} \times \vec{B} \right| \ll \left| q\vec{E} \right|$). Therefore any initial angle deviation from the normal direction immediately disappears. In our simulation, the electric field is around several hundred KV/m in zone1, zone2 and zone3 and the magnetic field magnitude is 8 orders less than the electric field magnitude. So, the electric field will play a dominant role during the initial emission stage. Because of

this, it is expected that our simulation results do reflect the true physical process despite our limited selection of perpendicular emission. However, in case of MP in a high magnetic field region, the initial angle effect is important and must be considered.

The secondary emission yield can be enhanced due to the glancing incident. This effect should be included in the analysis if measured SEY curves with glancing incident angles are available. The impact angle effect is not included in ACE3P at the moment.

VI. CONCLUSION

Simulations of MP in HOM couplers of the ILC and CEBAF 12 GeV upgrade cavities have been carried out with the 3D code of Omega 3P and Track 3P developed by SLAC. For the ILC cavity, resonant MP electron trajectories exist from 0.6 to 1.6 MV/m in Zone 1, 21 to 34 MV/m in Zone 2, 32 to 35 MV/m and above 40 MV/m in Zone 3. It is predicted that Zone 3 MP in an ILC cavity may limit the achievable gradient. Therefore, new HOM coupler designs are needed in further raising the gradient for the 1 TeV upgrade of the ILC. For the CEBAF 12 GeV upgrade cavity, resonant MP electron trajectories exist from 6 to 13 MV/m/ in Zone 1. This predicted MP barrier was not observed during the vertical cavity testing. It would be interesting to further assess this predicted barrier in the case of cavity operation with beam. The frequency scaling of Zone 1 and Zone 3 MP over a broad frequency range is found well correlated with the two-surface MP predicted by the simple parallel plate model. The scaling law provides the possibility of assessing MP behaviors in a TESLA-style HOM coupler by only examining the local electromagnetic fields. Such a possibility allows rapid iterations in future HOM coupler design efforts for SRF cavities.

References

[1] P.T.Farnsworth, J. Franklin Institute, 218, 411(1934).
[2] A.J.Hatch and H.B.Williams, J. Appl. Phys., 25, 417 (1954).
[3] C.M. Lyneis, H.A. Schwettman, J.P. Turneaure, Appl. Phys. Lett. , 31, 541 (1977).
[4] R.L. Geng, in Proceedings of the Particle Accelerator Conference, Lübeck, Germany, (2003), TOPB002, p264-268.
[5] Practically, a hard MP barrier refers to a barrier that cannot be overcome by using the processing technique. Physically, a hard MP barrier is characterized by resonant trajectories with high phase stability and an impact energy in the range of 100-1000 eV. These conditions ensure a SEY larger than unity even for a clean surface and exponential growth in electron density which ultimately leads to RF breakdown.
[6] U. Klein and D. Proch, Proceedings of the Conference on Future Possibilities for Electron Accelerators, (1979), N1-17.

[7] P. Kneisel et al., Nucl. Instrum. Methods Phys. Res., 188, 669, (1981).

[8] J. Sekutowicz, in Proceedings of the 6th Workshop on SRF. Virginia, USA, (1993), SRF93G04, P426-439.

[9] R.L. Geng et al., in Proceedings of the XXIV Linear Accelerator Conference, Victoria, British Columbia, Canada, (2008), THP042, p879-881.

[10] G. Kreps et al., in Proceedings of the 14th International Conference on RF Superconductivity, Berlin, Germany, (2009), TUPPO036, p289-291.

[11] A. Yamamoto, in Proceedings of the XXVI Linear Accelerator Conference, Tel-Aviv, Israel, (2012), HT3A01, p787-791.

[12] I.Gonin, N. Solyak, et al, in Proceedings of the Particle Accelerator Conference, New Mexico, USA, (2007), WEPMN093, p2248-2250.

[13] L.S. Cardman and L. Harwood, in Proceedings of the Particle Accelerator Conference, Albuquerque, New Mexico, USA, (2007), MOZBKI0, p58-62.

[14] C.E. Reece, et al., in Proceedings of the 13th International Conference on RF Superconductivity, Beijing, China, (2007), WEP31, p536-539.

[15] F. Marhauser, in Proceedings of the International Workshop on HOM Damping in Superconducting RF Cavities, Cornell university, 2010, [http://www.lns.cornell.edu/Events/HOM10/Agenda.html].

[16] F. Marhauser, A. Burrill, et al, in Proceedings of the 2th International Particle Accelerator Conference, San Sebastián, Spain, (2011), MOPC112, p337-339.

[17] Sang-ho Kim, I. E. Campisi, et al, in Proceedings of the 2006 Linear Accelerator Conference, Knoxville, Tennessee USA, (2006), THP081, p770-772, [http://accelconf.web.cern.ch/AccelConf/l06/PAPERS/THP081.PDF].

[18] K. Ko et al, in Proceedings of the 2010 Linear Accelerator Conference, Tsukuba, Japan, (2011), FR101, p1028-1032.

[19] L. Ge, Z. Li, et al, in the proceeding of IPAC 2012, Louisiana, USA, (2006),WEPPC068, p 2366-2368.

[20] C. Ng, V. Akcelik, et al, in the proceeding of EPAC 2006, Edinburgh, Scotland, (2006), THXFI01, p2763-2767.

[21] Z. Li of SLAC, private communication (2013).

[22] Padamsee H, Knobloch J, Hays T. RF Superconductivity for Accelerators. New York: John Wiley & Sons, Inc., 1998. 184

[23] G. Wu, H. Wang, et al, in Proceedings of the 12th International Workshop on RF Superconductivity, Ithaca, New York, USA, (2005), THP58, p600-603.

[24] Thomas P. Wangler, RF Linear Accelerators. Wiley-VCH Verlag GmbH & Co. KGaA, 2008, 159-161.

[25] D. Kostin, J. Sekutowicz, et al, in Proceedings of the 15th International Workshop on RF Superconductivity, Chicago, USA, (2011), THPO003, p691-694.

[26] D. Reschke et al., in Proceedings of the 15th International Workshop on RF Superconductivity, Chicago, USA, (2011), THPO046, p490-494.

[27] T. Khabiboulline, I. Gonin, et al, in Proceedings of the Particle Accelerator Conference, New Mexico, USA, (2007),WEPMN098, p2259-2261.